Chin. J. Astron. Astrophys. Vol. 1, No. 1, (2001) 21–28
(http://www.chjaa.org or http://chjaa.bao.ac.cn)

Chinese Journal of Astronomy and Astrophysics

LETTERS

Origin and Properties of Strong Mg II Quasar Absorption Line Systems

Wei-Peng Lin[1,2,3] ⋆ and Zhen-Long Zou[1,2]

[1] Beijing Astronomical Observatory, Chinese Academy of Sciences, Beijing 100012
[2] CAS-Peking University Joint Beijing Astrophysical Center, Beijing 100871
[3] Shanghai Astronomical Observatory, the Partner Group of MPI für Astrophysik, Shanghai 200030

Received 2000 December 12; accepted 2000 December 15

Abstract Strong Mg II quasar absorption line systems provide us with a useful tool to understand the gas that plays an important role in galaxy formation. In this paper, placing the theories of galaxy formation in a cosmological context, we present semi-analytic models and Monte-Carlo simulations for strong Mg II absorbers produced in gaseous galactic haloes and/or galaxy discs. We investigate the redshift path density for the Mg II absorption lines and the properties of galaxy/absorber pairs, in particular the anti-correlation between the equivalent width of Mg II absorption line and the projected galaxy-to-sightline distance. The simulated result of the mean redshift path density of strong Mg II systems is consistent with the observational result. The fraction of strong Mg II systems arising from galaxy disks is predicted to be $\sim$ 10% of the total. There exists an anti-correlation between the absorption line equivalent and the projected distance of sightline to galaxy center and galaxy luminosity. We determined that the mean absorbing radius $R_{\rm abs} \approx 29\,h^{-1}\,{\rm kpc}(L_B/L_{B*})^{0.35}$. After taking selection effects into consideration, this becomes $R_{\rm abs} \approx 38\,h^{-1}\,{\rm kpc}(L_B/L_{B*})^{0.18}$, which is in good agreement with the observational result. This shows the importance of considering selection effects when comparing models with observations.

Key words: galaxies:formation–galaxies: fundamental parameters–galaxies: haloes–quasars: absorption lines

1 INTRODUCTION

In the literature, metal absorption lines in quasar spectra are thought to originate in gaseous galactic haloes (Bahcall et al. 1969). Strong Mg II absorbers are of this kind (see Steidel 1998 for a review). On the observational side, strong Mg II absorbers at low redshift were inferred to be associated with massive halos in normal luminous galaxies (Petitjean & Bergeron 1990), and there have been clear clues that Mg II host galaxies are of various morphological

⋆ E-mail: linwp@bac.pku.edu.cn

types and over a large range of luminosities and possessing gaseous envelopes with an average radius of many tens of kpc(Steidel 1995). This radius is within the radius of the so-called "dark matter halo" of the galaxy. On the theoretical side, there are models dealing with such absorption line systems. For example, Mo & Miralda (1996) suggest that strong Mg II systems are produced by gaseous galactic haloes in analogy with the Lyman Limit systems. Considering absorption by clouds in galactic haloes, galaxy disks and dwarf satellites, Lin, Börner and Mo (2000) used semi-analytical methods and Monte-Carlo simulations to study the low redshift Lyα absorbers associated with galaxies. In this kind of models, the galaxy is thought to possess a gaseous envelope which can be totally parameterized in the context of cosmogony by the gravitational potential of the host dark matter halo, the cooling flow as well as the cosmic UV background ionizing field. Charlton & Churchill (1996; 1998) argued that galaxy disks might also be potential absorbers and they constructed a simple model to explain the kinematics of Mg II absorption line profiles. There is little doubt that gas in disks is involved in the absorption, since low ionized ions trace the HI distribution and there are large amounts of HI in galaxy disks. In fact, roughly 10% of the Mg II systems are also damped Lyman α absorbers (with very high HI column densities). However even from up-to-date observations, one cannot be sure of the geometry of the absorbers, whether it is spherical or disk-like. Nevertheless, it is reasonable that the Mg II absorbers should originate both in clouds in the halo and in the gas of the disk. In this paper we shall apply similar methods as in Lin et al. (2000), but with specific emphasis on strong Mg II absorption by clouds in galaxy halo and disk, and study the properties of strong Mg II system, particularly, the gas-cross section (or the absorbing radius), the number of absorbers per unit redshift and the anti-correlation of the equivalent width versus the galaxy-to-sightline distance in projection.

The models and simulations give reasonable redshift path density for strong Mg II systems and predict that the radius of the absorbing galaxy depend on its luminosity in the form, $R_{\rm abs} \approx 29\,h^{-1}\,{\rm kpc}(L_B/L_{B*})^{0.35}$. This is the first time for models to predict such a relationship. If we take into account the selection effects (e.g., apparent magnitude limit, absorption line width low limit, etc.), the dependence becomes $R_{\rm abs} \approx 38\,h^{-1}\,{\rm kpc}(L_B/L_{B*})^{0.18}$. The latter is in good agreement with the observational result.

The layout of this paper is as follows. The methods of the simulations are summarized in Section 2. In Section 3, we present the results of the simulations. Section 4 presents a discussion and conclusions. Throughout the paper, we adopt a dimensionless Hubble constant $h = H_0/(100\,{\rm km\,s^{-1}\,Mpc^{-1}})$. Our calculation is based on the ΛCDM cosmology (with $\Omega_0 = 0.3$, $\Lambda = 0.7$).

2 THE MONTE-CARLO SIMULATIONS

The Monte-Carlo galaxy sample used in the paper is generated from the luminosity function of field galaxies, about 70% of which are spirals galaxies and 30% of which are ellipticals. We use the luminosity function from the AOTUFIB redshift survey (Ellis et al., 1996) over the redshift interval $0.02 < z < 0.15$, which is expressed in the Schechter form, $\phi(L_B) = \phi^*(L_B/L_{B*})^{-\alpha}\exp(-L_B/L_{B*})d(L_B/L_{B*})$ with $\phi^* = 2.45 \times 10^{-2}h^3\,{\rm Mpc}^{-3}$, $M_{B*} = -19.30$, and $\alpha = 1.16$. $L_{B\rm min}$, the minimum B-band luminosity, is about $0.01L_{B*}$. The sample galaxies are placed randomly within a cylindrical volume in co-moving coordinates along the line-of-sight (hereafter LOS) toward a given QSO at redshift z_q. We consider those galaxies in a cylinder within a radius of $R_{\rm cy} = 400h^{-1}\,{\rm kpc}$ centered on the LOS. The number of galaxies at redshift

z in interval Δz is

$$\Delta N_{\rm g} = n_c(1+z)^3 \pi R_{\rm cy}^2 \frac{cdt}{dz}\Delta z, \qquad 0 < z < z_{\rm q}, \tag{1}$$

where $\frac{dt}{dz} = \frac{1}{(1+z)H(z)}$, and $H(z) = H_0[\Omega_\Lambda + (1-\Omega_\Lambda-\Omega_0)(1+z)^2 + \Omega_0(1+z)^3]^{1/2}$. The co-moving galaxy density n_c is the integration of the luminosity function $\phi(L_B)$. The luminosities of these galaxies are selected in such a way that their distribution is consistent with the luminosity function $\phi(L_B)$.

At any given epoch, a halo can be parameterized by the circular velocity $V_{\rm cir}$, which is simply related to the morphological type and luminosity of the galaxy. Empirical relations are known between the B-band magnitude and the LOS velocity dispersion, σ, of the matter in the galaxy both for ellipticals and spirals (Faber & Jackson 1976; Tully & Fisher 1977).

The Faber-Jackson relation is

$$-M_B + 5\log h = (19.39 \pm 0.07) + 10(\log\sigma - 2.3) \tag{2}$$

for ellipticals, and

$$-M_B + 5\log h = (19.75 \pm 0.07) + 10(\log\sigma - 2.3) \tag{3}$$

for S0's (Fukugita & Turner 1991). The circular velocity of the halo for elliptical and S0 galaxies is $V_{\rm cir} = \sqrt{2}\sigma$.

For spirals the Tully-Fisher relation is used to derive the LOS velocity width Δv. We take (Fukugita & Turner 1991)

$$-M_B + 5\log h = (19.18 \pm 0.10) + (6.56 \pm 0.48)(\log\Delta v - 2.5). \tag{4}$$

The halo circular velocity for a spiral is $V_{\rm cir} = \Delta v/2$.

Once we get the circular velocity of a galaxy, we model the gaseous halo following the work of Mo & Miralda-Escudé (1996). It was assumed that the gas in a halo has a two-phase (a hot phase and a cold phase) structure which, in principle is described by the density and temperature profiles. The density profiles are characterized by the so-called cooling radius and virial radius. And the temperature of the hot gas is characterized by the virial temperature.

In cooling flow models, a self-similar density profile for hot gas is assumed to be,

$$\rho_h(r) = \rho_h(r_c)\frac{2r_c^2}{r(r+r_c)}, \tag{5}$$

where

$$\rho_h(r_c) = \frac{5\mu k T_v}{2\Lambda(T_v)t_{\rm M}}. \tag{6}$$

We also assume

$$\rho_h(r_c) = \frac{f_g V_{\rm cir}^2}{4\pi G r_c^2}, \tag{7}$$

so that the density of the hot gas at this radius is a fraction f_g of the total density of the halo. $\Lambda(T_v)$ is the cooling rate of the gas at the virial temperature. The gas mass fraction f_g is assumed to be ~ 0.05 in this paper. μ is the average mass per particle, which is $\sim 0.6 m_{\rm H}$, $m_{\rm H}$ being the mass of hydrogen nucleus. The cooling radius r_c is determined by Eq. (6) and Eq. (7) to be $r_c = \sqrt{\frac{f_g\Lambda(T_v)t_{\rm M}}{5\pi G\mu^2}}$. The hot gas is taken to be isothermal, so that $T_h(r) \equiv T_v = \mu V_{\rm cir}^2/2k$. $t_{\rm M} = t/(1+\Omega_0)$, is the time interval between major mergers, since the gas is then shock heated to a stage from which it starts cooling. The cooling function $\Lambda(T_v)$ is adopted from Sutherland

& Dopita (1993). The age of a halo at redshift z_1 is $t = \int_{z_1}^{\infty} \frac{1}{(1+z)\,H(z)} dz$. The virial radius is $r_v = V_{\rm cir}/[10H(z)]$.

When the hot gas is shock heated and starts to cool, it will form cold clouds and sink to the center of the galaxy with a terminal velocity v_c which is of the same order of magnitude as $V_{\rm cir}$. We use $v_c = 0.5V_{\rm cir}$ for simplicity. Assuming spherical symmetry for the gas distribution, we can write the density of the cold gas as (see Mo & Miralda-Escudé 1996 for more details),

$$\rho_c(r) = \frac{f_g V_{\rm cir}^2 r_{\rm min}}{4\pi G t_{\rm M} r^2 v_c} \left[1 - \frac{r_{\rm min}^2}{r_c^2} \int_0^1 x^2 \bar{\rho_h}(x) dx\right], \tag{8}$$

where $r_{\rm min} = \min(r_v, r_c)$.

For simplicity, the cold gas is assumed to be in spherical clouds with masses constrained by various physical processes, such as gravitational instability, evaporation by hot gas, hydrodynamic instability, etc. Too large clouds will eventually collapse to form stars and too small clouds will evaporate by heat conduction and also be disrupted by hydrodynamic instabilities. As in Mo & Miradal-Escudé (1996), we use the mean mass of stable clouds, which is about $5 \times 10^5 M_\odot$. These clouds are confined by pressure of the hot medium, so that $\rho_{\rm cloud} T_c = \rho_h T_h$, where T_c, the temperature of the clouds, is about $2 \times 10^4 K$ (which is determined by the cooling function). The cloud radius is $R_c = (3M_c/4\pi\rho_{\rm cloud})^{1/3}$. The total hydrogen column density through the cloud center will be $N_0({\rm H}) = R_c \rho_{\rm cloud}/2.3\mu$, and the H number density is $n({\rm H}) = \rho_{\rm cloud}/2.3\mu$.

We assume that the cloud is almost completely photoionized by a constant UV background, and in ionization equilibrium. The fraction of hydrogen in the neutral state (HI atom), is determined by the flux of the UV background ionization field $J(\nu)$ and $n_{\rm H}$. We take

$$J(\nu) = J_{-21}(z) \times 10^{-21} \left(\frac{\nu}{\nu_{\rm HI}}\right)^{-\alpha} \times \Theta(\nu) {\rm erg\,cm^{-2} sr^{-1} Hz^{-1}\,s^{-1}}, \tag{9}$$

where $\nu_{\rm HI}$ is the hydrogen Lyman limit frequency, $J_{-21}(z) = 0.5$ for $z > 2$, and $J_{-21} = 0.5 \times [(1+z)/3]^2$ for $z < 2$. A break in the spectrum at $\nu_4 \equiv 4Ry$ (due to continuum absorption by He II), with $\Theta(\nu < \nu_4) = 1$ and $\Theta_4 \equiv \Theta(\nu \geq \nu_4) = 0.1$, is included (cf. Miralda-Escudé & Ostriker 1990; Madau 1992). We take $\alpha = 0.5$.

For $N({\rm H}) \leq 10^{19}$ cm^{-2}, which is the case for most clouds, the cloud is optically thin to the ionizing field with ionization parameter $U = \frac{\Phi({\rm H})}{n({\rm H})c}$, where the ionizing photon flux $\Phi({\rm H}) = \int_{\nu_{\rm HI}}^{\infty} \frac{4\pi J(\nu)}{h\nu} d\nu$. The neutral hydrogen column density $N_{\rm HI}$ can be derived from the code CLOUDY 90 (Ferland 1996). Using CLOUDY, we can derive the Mg II column density from the ratio of $N_{\rm Mg\,II}/N_{\rm HI}$ as a function of the ionization parameter U (cf. Fig.3 in Mo & Miralda-Escudé, 1996). Then we obtain the Mg II column density of a cloud at a distance to the LOS l, $N_{\rm Mg\,II} = N_{\rm Mg\,II}(0)\sqrt{1 - l^2/R_c^2}$, where $N_{\rm Mg\,II}(0)$ is the HI column density through the cloud center.

As mentioned above, galaxy disks may contribute to some absorption. We model the galaxy disk as a thin disk in centrifugal balance and has an exponential surface density profile. The disk model follows Mo, Mao & White (1998). The gas in the disk is ionized by the cosmic UV ionizing field incident from both sides of the disk. The HI in such a disk has a "sandwich structure", that is, in the central part of the disk, almost all the hydrogen is in the HI phase, and there is an HII region above the HI layer. This HI layer extends to some distance where the HI column density drops sharply and then the HI layer disappears ("the sharp edge" of the HI disk). The calculation of HI column density of the disk is straight forward (but refer to Lin et al. 2000, for details). As we know the HI column density, again the Mg II column density can be calculated using CLOUDY 90.

There might be one or more absorbing clouds in the LOS with different velocities with respect to the galaxy center. Assuming a Voigt profile for each absorbing component, the optical depth of a single line is $\tau_\nu \approx 2.65 \times 10^{-2} f_{jk} N_j \phi(\nu; \nu_{j,k})$ for $h\nu_{jk} \ll kT$, where f_{jk} is the oscillator strength of the line and N_j is column density, ϕ is the Voigt profile, j, k are the lower and upper energy level indexes, respectively. The rest frame equivalent width (hereafter REW), defined in frequency units is $W = \int (1 - e^{-\tau_\nu}) d\nu$. In accordance with observational usage, W is defined in wavelength units, so the value must be multiplied by λ/ν. We use the Mg II line, $\lambda = 2796.352$Å, $f_{jk} = 0.592$. Integrating over the velocity structure corresponding to the several absorbing clouds, the overall rest-frame equivalent width can be calculated.

To get statistically meaningful results, we simulate with 200 line of sights each of which covers the redshift span from 0 to 1. The procedure above produces a catalogue of absorber-galaxy pairs with information for further analysis.

3 THE PROPERTIES OF STRONG Mg II SYSTEMS

Our model predicted that dN/dz for $W_{\rm Mg\,II} \geq 0.3$ Å lines is about 0.51 (103 absorbers for 200 sightlines) averaged over the redshift span from 0 to 1. The strong Mg II systems are generally thought to be observational counterpart of the Lyman limit systems, for which $dN/dz = 0.5 \pm 0.3$ at $z = 0.5$ (Bahcall et al. 1996) and $dN/dz = 0.7 \pm 0.2$ at $\langle z \rangle = 0.7$ (Stengler-Larrea et al. 1995). Thus, our predicted dN/dz for strong Mg II systems is in good agreement with the observational results. And it is consistent with previous model predictions by Mo & Miralda-Escudé (1996), although their population of haloes were generated using the Press-Schechter model (Press & Schechter 1974) but not directly from luminosity function and they did not include galaxy disks. We also calculated the average dN/dz for separately for the redshift intervals from 0 to 0.5 and from 0.5 to 1.0, and the numbers are 0.55 and 0.48, respectively: there is no strong redshift evolution of dN/dz for strong Mg II systems in our simulation. This result is consistent with the observational results for redshifts < 1.

To answer the question how larger a fraction of strong Mg II systems arise from galactic haloes and how large from galaxy disks, we also simulate mock observation only considering absorption by disks, the outcome shows that $dN/dz \sim 0.05$, which is only $\sim 10\%$ of the dN/dz given above. This fraction is small and contradicts the inference of the empirical kinematics model (Charlton & Churchill, 1996; 1998). In that model, galaxy disks are inferred to be comparable to haloes in producing absorption line kinematics. However, observational results imply that the geometry of absorbing objects prefers to be spherical (cf. Steidel 1995). Since our predicted fraction of absorption by galaxy disks is relatively small, and the model will not violate the observational inference.

There exists an anti-correlation between the REW and the projected distance, namely $\log W_r = -\alpha \log \rho + \text{constant}$. The analysis shows, $\alpha \simeq 0.38 \pm 0.03$ and the constant is $\sim -0.05 \pm 0.05$. Fig. 1 shows the simulated result for galaxy-Mg II absorption line pairs with REW larger than 0.1 Å. The REW dependence on projected distance is not strong because the large scatter of galaxy properties (the large range of galaxy luminosities or circular velocities).

The REW may also depend on the galaxy luminosity. With all the simulated absorption line-galaxy pairs, a regression analysis of $\log W_r = -\alpha \log \rho + \beta \log(L_B/L_{B*}) + \text{constant}$ gives

$\alpha = 0.45 \pm 0.03$, $\beta = 0.16 \pm 0.03$, and the constant is 0.14 ± 0.06. As we can see, together with galaxy luminosity, the anticorrelation of REW on projected distance becomes stronger. Thus we can infer that the absorbing radius (REW ≥ 0.3 Å) of a galaxy with luminosity of L_B will be

$$R_{\rm abs} \approx 28.7\, h^{-1}\,{\rm kpc}(L_B/L_{B*})^{0.35}.$$

This "halo size/luminosity" relationship seems to match with the usual assumption that the gaseous size of galaxies would obey the Holmberg (1975) relation, $R_{\rm abs} \propto L^{0.4}$. The preliminary result of observations gave $R_{\rm abs} \approx 35\, h^{-1}\,{\rm kpc}(L_B/L_{B*})^{0.2}$ (Stedel 1995). However, the link of absorption line systems with luminous galaxies is subject to selection effects, namely, the limiting apparent magnitude in the galaxy surveys, the low limit of line equivalent widths, and the field of view. If we only use those galaxies in the mock survey with apparent B-band magnitude (see Lin et al. 2000 for detail) brighter than 24.3, and with REW larger than 0.1 Å, we get $\alpha = 0.61 \pm 0.05$, $\beta = 0.11 \pm 0.04$, and the constant is 0.44 ± 0.10 for the same analysis above. Fig. 2 shows the analysis, as we can see, faint absorbing galaxies (shown in Fig. 1) disappear, and the anti-correlation becomes stronger (the scatter also becomes smaller) than in Fig. 1. As a result of taking into account the selection effects, the average absorbing radius of a galaxy with luminosity L_B will be

$$R_{\rm abs} \approx 37.9\, h^{-1}\,{\rm kpc}(L_B/L_{B*})^{0.18}$$

for strong Mg II systems. Thus, we conclude that our result of mock survey including selection effects is consistent with the observational result and that the available observational result must have been biased by the selection effects.

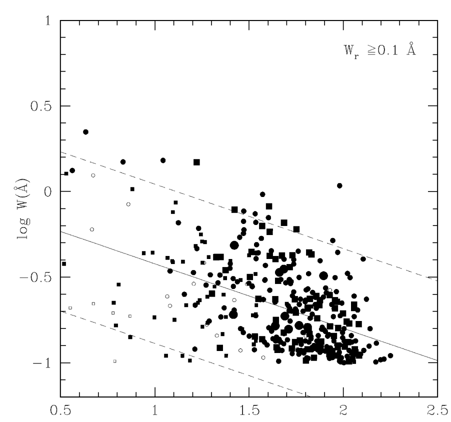

Fig. 1 The analysis of $\log W_r = -\alpha \log \rho +$ constant for bright galaxy-absorber pairs in the mock survey. The solid line is for the linear fit. About 95.4% of the data points lie between the 2σ lines shown dashed. Squares and circles are for spiral galaxies and elliptical/S0 galaxies respectively. Small open symbols represent galaxies of luminosities $L_B \leq 0.1 L_{B*}$, small filled symbols, those of luminosities $0.1 L_{B*} < L_B \leq L_{B*}$, and large filled symbols represent galaxies of luminosities $L_B > L_{B*}$.

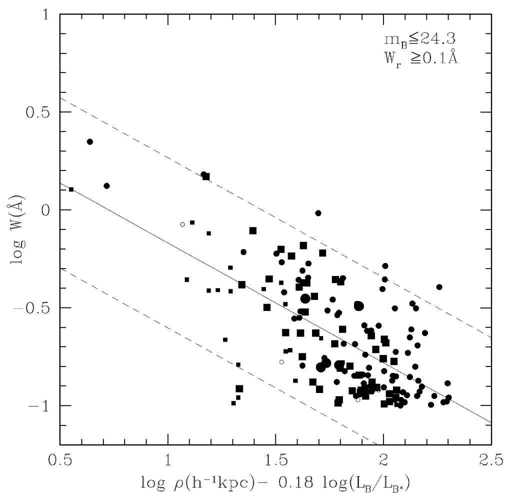

Fig. 2 Regression analysis of $\log W_r = -\alpha \log \rho + \beta \log(L_B/L_{B*})$ + constant for bright galaxy-absorber pairs in the mock survey. The meaning of various symbols and lines is the same as in Fig. 1.

4 SUMMARY AND DISCUSSION

Our simulated results show that strong Mg II absorption systems at $z < 1$ are closely related to luminous galaxies. There are two basic facts to support this conclusion. One is the observational redshift path density of the absorption systems can be reproduced by the simulations. The other is that there is an anti-correlation between the REW and projected distance together with the galaxy luminosity. The anti-correlation is natural in that the closer of the sightline to the galaxy center, the larger the total column density (hence the stronger the absorption line). We also study the selection effect when determining the relationship between the absorbing radius and luminosity of the galaxy. As we can see, selection effects can weaken the dependence of the absorbing radius on the luminosity because too faint galaxies were omitted in optical image surveys and that the absorbing radius of these faint/small galaxies may decrease more quickly with decreasing luminosity than that of the brighter/bigger galaxies (see Fig. 10 in Mo & Miralda-Escudé 1996).

The observational result used above is provided by Steidel (1995) which was based on only part of his survey. The total redshift path and the galaxy-absorber sample is still rather small and the result is preliminary. The whole survey is about to be finished. We are looking forward to seeing the final result of the survey which may provide us more information to study the selection effects and set constraints on the models.

Future work will study the reconstruction of luminosity function from gas-cross-section selected galaxies and the kinematics of low ionization metal (e.g., Mg II , Si II) absorption line systems; these will provide additional information on the absorbing gas and will place more constraints on the models. Other kinds of absorbing sources, for example, galactic winds, tidal tails, satellite galaxies, should also be studied and discussed in detail in the future.

Acknowledgments The authors thank Dr H.J. Mo for stimulating discussions. We thank Profs. Deng Zu-Gan, Wu Xiang-Ping for carefully reading the manuscript and important comments. WPL gratefully acknowledges the fellowship under the MPG-CAS exchange program.

References

Bahcall J. N., Spitzer L., 1969, ApJ, 156, L63
Bahcall J. N. et al., 1996, ApJ, 457, 19
Bergeron J., Boissé P., 1991, A&A, 243, 344
Bergeron J., Cristiani S., Shaver P., 1992, A&A, 257, 417
Charlton J. C., Churchill C. W., 1996, ApJ, 465, 631
Charlton J. C., Churchill C. W., 1998, ApJ, 499, 181
Ellis R. S., Colless M., Broadhurst T., Heyl J., Glazebrook K., 1996, MNRAS, 280, 235
Faber S. M., Jackson R. E., 1976, ApJ, 204, 668
Ferland G. J., 1996, Hazy, a Brief Introduction to Cloudy, University of Kentucky, Department of Physics and Astronomy Internal Report
Fukugita M., Turner E. L., 1991, MNRAS, 253, 99
Holmberg E., 1975, In: A. Sandage, M. Sandage, J. Kristian eds., Stars and Stellar Systems, Vol.9, Galaxies and the Universe, Chicago: Univ. Chicago Press, 123
Lin W. P., Börner G., Mo H. J., 2000, MNRAS, 319, 517
Madau P., 1992, ApJ, 389, L1
Miralda-Escudé J., Cen R., Ostriker J. P., Rauch M., 1996, ApJ, 471, 582
Miralda-Escudé J., Ostriker J. P., 1990, ApJ, 350, 1
Mo H. J., 1994, MNRAS, 269, L49
Mo H. J., Mao S., White S. D. M., 1998, MNRAS, 295, 319 (MMW)
Mo H. J., Miralda-Escudé J., 1996, MNRAS, 469, 589
Petitjean P., Bergeron J., 1990, A&A, 231, 309
Press W. H., Schechter P., 1974, ApJ, 187, 425
Steidel C. C., 1995, In: G. Meylan ed., QSO Absorption Lines, Berlin: Springer, 139
Steidel C. C., 1998, In: D. Zaritsky, ed., ASP Conference Series #136, Galactic Halos: A UC Santa Cruz Workshop, 167
Sutherland R. S., Dopita M. A., 1993, ApJS, 88, 253
Tully R. B., Fisher J. R., 1977, A&A, 54, 661